JOURNAL OF GEOPHYSICAL RESEARCH, VOL. 85, NO. C3, PAGES 1591–1599, MARCH 20, 1980

Determination of the Complex Refractive Index and Size Distribution of Atmospheric Particulates From Bistatic-Monostatic Lidar and Solar Radiometer Measurements

J. A. REAGAN, D. M. BYRNE,[1] M. D. KING,[2] J. D. SPINHIRNE,[2] AND B. M. HERMAN

University of Arizona, Tucson, Arizona 85721

A method is presented for inferring both the size distribution and the complex refractive index of atmospheric particulates from combined bistatic-monostatic lidar and solar radiometer observations. The basic input measurements are spectral optical depths at several visible and near-infrared wavelengths as obtained with a solar radiometer and backscatter and angular scatter coefficients as obtained from a bistatic-monostatic lidar. The spectral optical depth measurements obtained from the radiometer are mathematically inverted to infer a columnar particulate size distribution. Advantage is taken of the fact that the shape of the size distribution obtained by inverting the particulate optical depth is relatively insensitive to the particle refractive index assumed in the inversion. Bistatic-monostatic angular scatter and backscatter lidar data are then processed to extract an optimum value for the particle refractive index subject to the constraint that the shape of the particulate size distribution be the same as that inferred from the solar radiometer data. Specifically, the scattering parameters obtained from the bistatic-monostatic lidar data are compared with corresponding theoretical computations made for various assumed refractive index values. That value which yields best agreement, in a weighted least squares sense, is selected as the optimal refractive index estimate. The results of this procedure applied to a set of simulated measurements as well as to measurements collected on two separate days are presented and discussed.

1. INTRODUCTION

Accurate determinations of the size distribution and refractive index of atmospheric particulates are important for both environmental monitoring and radiative transfer studies. For example, atmospheric visibility and radiative transfer properties depend very strongly on the size distribution and optical properties of the particles present in the atmosphere. This is due to the fact that slight alterations in the optical properties or in the number of particulates in the atmosphere can influence the complicated energy budget of the earth-atmosphere system. Solid and liquid particles suspended in the atmosphere may also affect the optical and microphysical properties of clouds [*Twomey*, 1974, 1977; *Ackerman and Baker*, 1977], which in turn are suspected of having a profound influence on the basic climate of the earth. These sensitivities, coupled with the current lack of information about the properties of particulates in realistic atmospheres, make it extremely difficult to establish meaningful particulate emission standards or even to predict how the earth's climate may be perturbed by the injection of natural and man-made particles into the atmosphere.

Attempts to measure the size distribution and refractive index of particulates by direct means are complicated by the very small sizes and relatively sparse concentrations of particulates normally present in the atmosphere. For example, direct sampling methods that accumulate particles for subsequent analysis may produce results different from the particulate properties of the real atmosphere because of effects such as sampling line and collection surface biases, particle evaporation, and particle contamination. Other sampling methods may actually rely on indirect sensing techniques which require that the sampled particles meet certain constraints for the sampling system's calibration to be valid. To acquire above-ground, profile, or integrated height information about particulates by direct means also requires mounting a sampling system on a suitable platform such as an aircraft or balloon. This further complicates the process of relating the measured particulate properties to the properties of the actual particulates in the atmosphere.

Most of the aforementioned problems may be avoided by applying remote sensing techniques which permit sensing of the particulates in their natural surroundings. While remote sensing methods do present their own interpretation problems, a number of particulate remote sensing applications have already been demonstrated with apparently good success [e.g., *Yamamoto and Tanaka*, 1969; *Fernald et al.*, 1972; *Ward et al.*, 1973; *Russell et al.*, 1976; *Twitty et al.*, 1976; *Reagan et al.*, 1977*a*; *Spinhirne*, 1977; *Spinhirne et al.*, 1980; *King et al.*, 1978; *King*, 1979].

In the present investigation a procedure is developed for inferring the size distribution and both the real and the imaginary parts of the complex refractive index of atmospheric particulates from a combination of bistatic-monostatic lidar and solar radiometer measurements. An estimate of the columnar aerosol size distribution is first obtained by inversion of spectral optical depths which have been obtained by using a solar radiometer. Advantage is taken of the fact that the shape of the aerosol size distribution (i.e., relative variation of the particle number density with particle size) inferred from such measurements is quite insensitive to the particle refractive index assumed in the inversion. The refractive index is then derived from certain bistatic-monostatic lidar measurements which depend very strongly on the refractive index as well as the shape of the size distribution. Details of this procedure are presented and results are given for both simulated measurements and actual observations made on two separate days. (This paper is a revised and extended version of earlier conference papers [*Reagan et al.*, 1976, 1977*b*].)

[1]Now at United Technologies Research Center, West Palm Beach, Florida 33402.

[2]Now at NASA Goddard Space Flight Center, Greenbelt, Maryland 20771.

Paper number 9C1728.
0148-0227/80/009C-1728$01.00

2. THEORETICAL BASIS

Scattering and absorption of radiation by atmospheric particulates depend in a complex manner on the size distribution, shape, and refractive index (i.e., particle composition) of the aerosol particles. Assuming that atmospheric particulates can be modeled as a polydisperse collection of spherical particles with a single refractive index, the integral equation which relates the unit volume phase matrix elements $P_{ij}(\theta, \lambda)$ to the particle size distribution and refractive index may be written in the form

$$P_{ij}(\theta, \lambda) = \frac{1}{\beta_{ext}(\lambda)} \int_0^\infty \sigma_{ext}(r, \lambda, m) P_{ij}(r, \theta, \lambda, m) n(r)\, dr \qquad (1)$$

$$i, j = 1, 2, 3, 4$$

In this expression, $n(r)$ is the particulate number density in the radius range r to $r + dr$ (i.e., size distribution function), m the complex refractive index of the particles, λ the wavelength of the incident illumination, θ the scattering angle, $p_{ij}(r, \lambda, \theta, m)$ the ijth element of the single-particle scattering phase matrix, $\sigma_{ext}(r, \lambda, m)$ the single-particle extinction cross section, and $\beta_{ext}(\lambda)$ the unit volume extinction coefficient defined by

$$\beta_{ext}(\lambda) = \int_0^\infty \sigma_{ext}(r, \lambda, m) n(r)\, dr \qquad (2)$$

The phase matrix elements as defined here interrelate the F_l, F_r, F_u, and F_v Stokes components of the incident (i) and scattered (s) flux density, for single scattering by particulates in a unit volume of air, by the matrix expression

$$\begin{bmatrix} F_l \\ F_r \\ F_u \\ F_v \end{bmatrix}^s = \frac{\beta_{ext}}{R^2} \begin{bmatrix} P_{11} & 0 & 0 & 0 \\ 0 & P_{22} & 0 & 0 \\ 0 & 0 & P_{33} & P_{34} \\ 0 & 0 & -P_{34} & P_{44} \end{bmatrix} \begin{bmatrix} F_l \\ F_r \\ F_u \\ F_v \end{bmatrix} \qquad (3)$$

where R is the distance from the point of scattering to the point of observation. The element P_{11} characterizes scattering with the electric field component parallel (l) to the scattering plane, while P_{22} characterizes scattering with the electric field component perpendicular (r) to the scattering plane. The elements are normalized such that

$$\oint_{4\pi} \frac{(P_{11} + P_{22})}{2}\, d\Omega = \omega_0 \qquad (4)$$

where $d\Omega$ is the differential element of solid angle and ω_0 is the single-scattering albedo. For definitions and additional details regarding particle cross sections, Stokes parameters, and the scattering phase matrix the reader is referred to the works of *Chandrasekhar* [1960], *Deirmendjian* [1969], and *van de Hulst* [1957].

In the above formulation the aerosol is assumed to consist of homogeneous spherical particles characterized by a single refractive index with both real and imaginary components. The spherical particle assumption is made of necessity because there are presently no methods to tractably compute the scattering parameters for collections of randomly oriented irregularly shaped particles. Although the results of some experimental work [*Holland and Gagne*, 1970; *Pinnick et al.*, 1976; *Perry et al.*, 1978] indicate that there can be fairly large departures in the measured particle scattering parameters compared to those computed for spheres, the spherical particle assumption has been employed to obtain apparently good agreement between theory and observation in other studies [*Eiden*, 1966; *Grams et al.*, 1974; *Reagan et al.*, 1977*a*; *King*, 1979]. The assumption of a single refractive index, which is made in part to permit tractable calculations, has also been employed with apparent success in the analysis of several sets of observations [*Eiden*, 1966; *Ward et al.*, 1973; *Grams et al.*,1974; *Reagan et al.*, 1977*a*; *King et al.*, 1978]. Recognizing that actual atmospheric particulates are not all perfect spheres of a single refractive index, inferences of particle size and index made by analyzing radiation measurements subject to these assumptions must be regarded as 'effective particle' determinations. If such determinations yield scattering and absorption parameters which accurately characterize the radiation properties of the overall collection of particles in question, then the approach is indeed useful for radiative transfer studies.

Even after invoking the above two assumptions, efforts to invert (1) and (2) have, until recently, been limited to the retrieval of the aerosol size distribution with the refractive index assumed to be known [*Yamamoto and Tanaka*, 1969; *King et al.*, 1978] or the refractive index with the size distribution [*Grams et al.*, 1974] or form of the size distribution [*Ward et al.*, 1973; *Reagan et al.*, 1977*a*] assumed to be known. Optical techniques for determining both the size distribution and the index of absorption (i.e., imaginary component of m) of atmospheric particulates have been described by *King and Herman* [1979] and *King* [1979], using a combination of spectral optical depth and hemispheric flux density measurements, and *Spinhirne* [1977] and *Spinhirne et al.* [1980], using a combination of spectral optical depth and monostatic lidar normalized backscattering coefficient measurements. Attempts to retrieve both $n(r)$ and m are complicated by the fact that the size and refractive index dependencies in (1) and (2) cannot generally be separated or interrelated, even for spherical (Mie) particles. (When the real refractive index component is close to 1.0, *Yamamoto and Tanaka* [1969] showed analytically, using *van de Hulst*'s [1957] anomalous diffraction theory, that spectral extinction measurements are relatively insensitive to the particle refractive index and that the dependencies of r and m in the extinction coefficient are simply related. *King et al.* [1978] examined this result for refractive indices $m = n - \kappa i$ for which $1.45 \leq n \leq 1.54$ and $0.00 \leq \kappa \leq 0.03$ and came to the same conclusion.) The particular technique for determining $n(r)$ and m presented here is a sequential approach which combines bistatic-monostatic lidar and solar radiometer remote sensing methods previously developed by the authors [*Reagan and Herman*, 1970; *Reagan et al.*, 1977*a*; *Spinhirne*, 1977; *Spinhirne et al.*, 1980; *King et al.*, 1978].

From multiwavelength measurements of the directly transmitted solar flux density as a function of solar zenith angle, one can obtain spectral values of the total optical depth $\tau_t(\lambda)$ as described by *Shaw et al.* [1973]. Values of the particulate optical depth $\tau_p(\lambda)$ at selected wavelengths λ may then be determined from the total optical depth measurements by subtracting contributions due to molecular scattering and absorption (primarily due to ozone) as described by *King and Byrne* [1976].

The integral equation which relates optical depth to an aerosol size distribution can be written as

$$\tau_p(\lambda) = \int_0^\infty \sigma_{ext}(r, \lambda, m) n_c(r)\, dr \qquad (5)$$

where $n_c(r)$ is the columnar aerosol size distribution, that is, the number of particles per unit area per unit radius interval in a vertical column through the atmosphere. The columnar size distribution is related to the height-dependent aerosol size distribution $n(r, z)$ through the expression

$$n_c(r) = \int_0^\infty n(r, z)\, dz \tag{6}$$

If $n_c(r)$ is well approximated by a *Junge* [1955] distribution which extends over a fairly broad size range, then $n_c(r)$ may be determined by applying a simple curve-fitting technique to the $\tau_p(\lambda)$ data [*Shaw et al.*, 1973]. A more general solution for $n_c(r)$ may be obtained by mathematically inverting (5). In practice, the integral in (5) is approximated by a numerical summation to obtain a set of linear algebraic equations, one equation for each known value of $\tau_p(\lambda)$. The equations are then inverted numerically by matrix inversion techniques to solve for weighted solution points of the unknown distribution $n_c(r)$ as described by *King et al.* [1978]. It should be noted that the inversion for $n_c(r)$ does not depend on how the particles are spatially distributed in the column with regard to particle size or refractive index (i.e., there is no assumed constraint between $n_c(r)$ and $n(r, z)$). This technique has already been employed to extract aerosol size distributions from optical depth data for more than 60 days of University of Arizona solar radiometer observations.

A particularly attractive feature of spectral optical depth and volume extinction coefficient measurements is that they are relatively insensitive to the complex refractive index of the aerosol particles. This permits solutions of (2) and (5) for the aerosol size distribution which are not greatly affected by the value of the refractive index assumed in the inversion. The refractive index sensitivity which does exist is such that the inverted size distributions maintain their shape under various assumed values for the refractive index, shifting slightly in both magnitude and radius [*Yamamoto and Tanaka*, 1969; *King et al.*, 1978]. In addition, extinction and near forward scatter measurements are only weakly altered by particles which are irregularly shaped rather than spherical [e.g., *Hodkinson*, 1963; *Holland and Gagne*, 1970; *Zerull and Giese*, 1974]. As was discussed by *Pollack and Cuzzi* [1978], the extinction efficiency of polydispersions of randomly oriented irregular particles can be enhanced over that of spheres of equivalent volume by ~20–30% for particles with size parameters (i.e., particle circumference to wavelength ratios) greater than about 4. This discrepancy can apparently be largely scaled out by normalizing to spheres of equivalent surface area rather than equivalent volume [*Pollack and Cuzzi*, 1978]. Thus particle size distributions obtained by inverting $\tau_p(\lambda)$ data should not be significantly altered if the actual particles are not perfect spheres.

The phase matrix elements defined by (1) are, on the other hand, quite sensitive both to the size distribution and to the refractive index of the particulates (especially for scattering in the backward hemisphere). This sensitivity is utilized in the refractive index retrieval method which employs measurements of the $P_{11}(\theta, \lambda)$ and $P_{22}(\theta, \lambda)$ phase matrix elements, for various scattering angles, and the particulate extinction to backscatter ratio. One can obtain values of $P_{11}(\theta, \lambda)$ and $P_{22}(\theta, \lambda)$ from bistatic lidar measurements (at a fixed scattering angle and wavelength) of the radiation scattered by a volume of atmospheric air in planes parallel and perpendicular to the scattering plane defined by the transmitter and receiver axes, respectively [*Reagan and Herman*, 1970; *Byrne*, 1978]. This procedure requires determination of the molecular or Rayleigh component of the scattering cross section at the altitude of the scattering volume, together with an estimate of the transmission to the scattering volume altitude. The molecular scattering correction is obtained by measuring the light scattered from a volume of air which contains relatively few particulates. The altitude which is routinely chosen is 8 km. This represents a reasonable compromise between an altitude which is sufficiently high to yield a scattered signal due mostly to molecular scattering and an altitude which is not so high as to yield a scattered signal which is unacceptably small and noisy. Once the Rayleigh scattering cross section is determined for the reference altitude, it is scaled by the molecular number density profile to obtain the corresponding Rayleigh value at the lower altitude where the bistatic angular scan is normally made. The transmissions to the reference altitude and to the lower angular scan altitude are determined from concurrent monostatic lidar measurements by the slant path analysis procedure described by *Spinhirne* [1977] and *Spinhirne et al.* [1980]. By simultaneously varying the elevation angles of the lidar transmitter and bistatic receiver it is possible to obtain values of the phase matrix elements for a range of scattering angles at a fixed height above ground (i.e., a horizontal scan). The angular scattering range which is obtainable is a function of the height above ground of the scattering volume and the geometry of the lidar system. For the University of Arizona lidar system [*Reagan and Herman*, 1970] operating with the scattering volume 0.8 km above ground (which is a typical bistatic operating condition) the available range of scattering angles is $20° \leq \theta \leq 160°$ [*Byrne*, 1978]. Backscatter measurements ($\theta = \pi$) required to determine the transmissions to the reference and the horizontal angular scan altitudes are also made with this system by using the monostatic receiver mounted parallel and adjacent to the transmitter.

The particulate volume extinction to volume backscattering ratio $S(\lambda) = \beta_{ext}(\lambda)/\beta_{scat}(\pi, \lambda)$ can be written in terms of the phase matrix elements defined by (1) as

$$S(\lambda) = 2/[P_{11}(\pi, \lambda) + P_{22}(\pi, \lambda)] = 1/P_{11}(\pi, \lambda) \tag{7}$$

since $P_{11}(\theta, \lambda) = P_{22}(\theta, \lambda)$ for a scattering angle of $\theta = \pi$. This ratio may be obtained from multiangle slant path monostatic lidar measurements as described by *Spinhirne* [1977] and *Spinhirne et al.* [1980]. The slant path analysis technique extracts an integrated or columnar $S(\lambda)$ value over a selected height interval, typically the entire mixing layer, as well as $\beta_{ext}(\lambda)$ and $\beta_{scat}(\lambda, \pi)$ versus height. In applying this technique it is assumed that $S(\lambda)$ is constant with height over the altitude interval for which the solution is attempted. Some degree of horizontal homogeneity in the particulate optical properties is also required for accurate implementation of the technique (horizontal variations in $\beta_{scat}(\lambda, \pi)$ of 10–20% at a given height can be tolerated without apparent difficulty). The constraint that $S(\lambda)$ be constant with height requires that the refractive index and shape of the size distribution of the particulates remain constant with height. However, no assumptions regarding the specific particle refractive index value and size distribution form or the value of $S(\lambda)$ are required to implement the solution technique. The error levels in $\beta_{ext}(\lambda)$ and $S(\lambda)$ derived from the solution procedure reflect whether or not the requirements of horizontal homogeneity and S remaining constant with height are reasonably well met for a given set of slant path measurements. Results from many days of observations

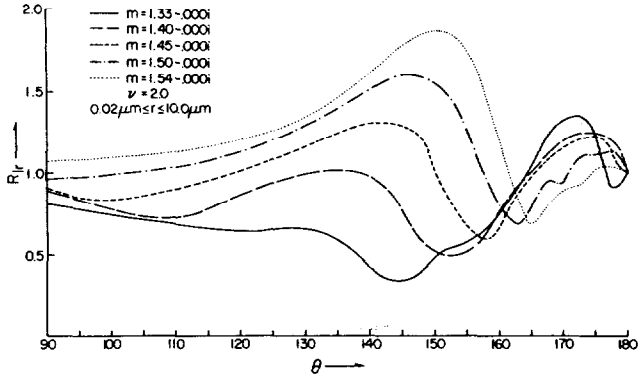

Fig. 1. Polarization ratio R_{lr} as a function of θ for $\nu = 2.0$ and for selected values of m ($\lambda = 0.6943$ μm).

reveal that $\beta_{ext}(\lambda)$ and $S(\lambda)$ can frequently be determined with an rms uncertainty between 10 and 20% [*Spinhirne*, 1977; *Spinhirne et al.*, 1980].

By using certain combinations of the above defined scattering and extinction parameters it is possible to formulate functions which are particularly sensitive to the complex refractive index of atmospheric particulates [*Eiden*, 1971]. For example, we have found that the particulate polarization ratio $R_{lr}(\theta, \lambda)$, defined by $R_{lr}(\theta, \lambda) = P_{11}(\theta, \lambda)/P_{22}(\theta, \lambda)$, is quite sensitive to the real component of m [*Reagan et al.*, 1977*a*]. This is shown graphically in Figure 1, where theoretically computed values of $R_{lr}(\theta, \lambda)$ are plotted as a function of θ for different real values of m and a Junge size distribution with $\nu = 2.0$ and a radius range extending from 0.02 to 10.0 μm. In these computations, as well as in all lidar computations to follow, the wavelength of the laser illumination is taken as 0.6943 μm (corresponding to the University of Arizona ruby lidar system), and the λ dependence is subsequently dropped from the lidar scattering parameter notation. The plots reveal a widely separated single-valued dependence on the real component of m for a fairly large angular scattering range. Similar calculations for different values of ν and m with nonzero imaginary components also yield curves that are well separated and single valued in the real component of m. There is also some sensitivity in $R_{lr}(\theta)$ to the imaginary component of m, but the sensitivity to the real component of m is generally more dominant.

It should be noted that the behavior of $R_{lr}(\theta)$ may be significantly altered if the particles are irregular in shape rather than spherical. Angular scattering measurements of the intensity and polarization characteristics of monodisperse and relatively narrow polydisperse collections of randomly oriented irregular particles clearly reveal large departures from the scattering properties of spheres for scattering angles θ greater than about 40° [*Holland and Gagne*, 1970; *Zerull and Giese*, 1974; *Zerull and Weiss*, 1976; *Pinnick et al.*, 1976; *Perry et al.*, 1978]. These measurements reveal that $P_{11}(\theta)$ and $P_{22}(\theta)$ are both generally enhanced (although not necessarily both by the same proportion) in relation to what they would be for spheres for the scattering range $\sim 40° < \theta < \sim 160°$. The effect is particularly significant around $\theta = \sim 120°$, where $P_{11}(\theta)$ and $P_{22}(\theta)$ can be enhanced by as much as a factor of ~5 in some cases. The enhancement is diminished for broader polydispersions, and irregular particles with effective size parameters less than ~5 do not yield scattering characteristics much different from those of spheres. The effect of irregular particles on $R_{lr}(\theta)$ is also lessened by the fact that $P_{11}(\theta)$ and $P_{22}(\theta)$ are both generally enhanced. Nevertheless, it must be recognized that measurements of $R_{lr}(\theta)$ for actual atmospheric particulates may not agree in some cases with theoretical computations based on equivalent spheres.

We have found the S ratio defined earlier also to be quite sensitive to m. This sensitivity is shown in Figure 2, where the S ratio is plotted as a function of ν for several values of m. It can be seen that S varies significantly with the imaginary as well as with the real refractive index component. An analysis of the refractive index sensitivity of the backscattering cross section indicates that when $\lambda = 0.6943$ μm, S is sensitive to the imaginary index component predominantly for particles which are of a radius greater than 1 μm [*Spinhirne*, 1977; *Spinhirne et al.*, 1980]. However, for particles smaller than 1 μm the dependence of S on the real part of m is more important. For a size distribution where scattering is primarily due to larger particles, such as the case of a Junge size distribution with $\nu = 2$, the resulting extinction to backscatter ratio is highly sensitive to the imaginary component of m. When scattering by smaller particles dominates, as it does for a Junge size distribution with $\nu \geq 3$, the dependence of S on the imaginary component of m is not as pronounced.

Experimental measurements have indicated that S, or alternatively, the phase function at $\theta = \pi$, is also sensitive to particle shape [*Pinnick et al.*, 1976]. Nonspherical particle scattering effects have been found to decrease the volume backscattering coefficient from that which would be expected for equivalent spheres. Since increasing the imaginary component of the index of refraction also decreases the backscattering coefficient, values of the imaginary component inferred for actual atmospheric particulates by optical backscattering techniques should be upper limits to the true values of the imaginary component. The results given in this paper should be so interpreted, but given the current lack of knowlege of the refractive index of atmospheric particulates, such results are nevertheless useful.

Kuriyan et al. [1974] and *Fymat* [1976] have investigated the feasibility of using ratios of visible wavelength particulate optical depths $(\tau_p(\lambda_i)/\tau_p(\lambda_j))$ to infer the particulate refractive index. Results of their calculations indicate that these ratios must be measured with extremely, perhaps unrealistically,

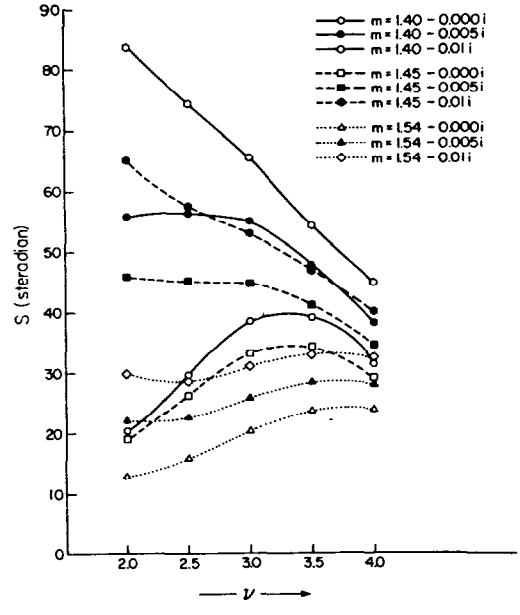

Fig. 2. Extinction to backscatter ratio S as a function of $\nu = 2.0$ and for selected values of m ($\lambda = 0.6943$ μm).

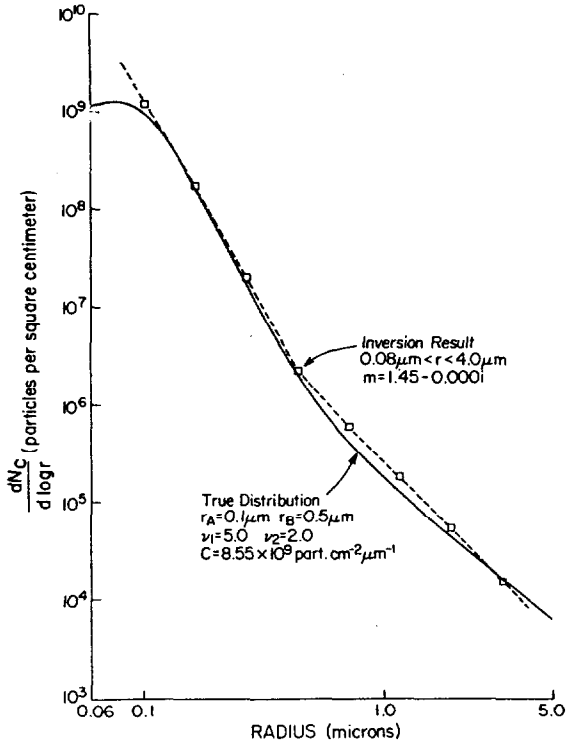

Fig. 3. Inversion solution for simulated $\tau_p(\lambda)$ data calculated for a refractive index of $m = 1.50 - 0.005i$ and a two-slope model size distribution extending in radius from 0.02 to 10.0 μm.

good accuracy to obtain very accurate estimates of m. This is not surprising considering the weak sensitivity of spectral extinction measurements to particulate refractive index (at least for $1.45 \leq n \leq 1.54$ and $0.00 \leq \kappa \leq 0.03$), as was noted earlier in this paper and discussed by *King et al.* [1978]. The ratio parameters $R_{l_r}(\theta)$ and S appear to be significantly more sensitive to variations in m than the optical depth ratios.

The procedure that we have developed for quantitatively estimating the refractive index from measurements of $R_{l_r}(\theta)$ and S is to compare the measurements with computations of the same functions made for various values of m with the constraint that the size distribution used for these calculations be that obtained by inverting the $\tau_p(\lambda)$ data. As was indicated previously, a numerical inversion of (5) is performed to obtain an estimate of the columnar particle size distribution $n_c(r)$. This estimate of $n_c(r)$ is then used to calculate $R_{l_r}(\theta)$ and S for an assumed value of m. This procedure is repeated, using the same columnar size distribution but different values for the refractive index.

To determine the value of m which optimally describes a particular set of measurements, a performance function is formulated which indicates the agreement in a least squares sense between the experimental data and the values which were computed by using the columnar size distribution and the assumed refractive index. The performance function used here is given by

$$Q(m) = \frac{1}{2}\left\{\frac{1}{N}\sum_{i=1}^{N}\left[\frac{R_{l_r}{}^{C}(\theta_i, m) - R_{l_r}{}^{E}(\theta_i)}{R_{l_r}{}^{E}(\theta_i)}\right]^2\right\} + \frac{1}{2}\left[\frac{S^C(m) - S^E}{S^E}\right]^2 \quad (8)$$

where the superscripts C and E denote calculated and experimentally determined quantities, respectively, and the θ_i are the scattering angles for which $R_{l_r}{}^{E}$ data are available. Because S and $R_{l_r}(\theta)$ are both ratios, no scaling difficulties are encountered in using the columnar size distribution $n_c(r)$ instead of the height-dependent particle size distribution $n(r, z)$. As can be shown by using (6), these two particle size distributions differ by only a constant scaling factor if the form of the size distribution as a function of particle radius is independent of height z. The performance function given by (8) is composed of equally weighted terms corresponding to the average squared fractional difference between experimental and calculated polarization ratios and the squared fractional difference between experimental and calculated S ratio values. The optimum refractive index is selected to be the value of m which yields the smallest value of $Q(m)$, (i.e., value of m yielding the best fit between the experimental measurements and the theoretical computations).

The values of m typically used in the fitting library include real components of 1.33, 1.40, 1.45, 1.50, and 1.54 and imaginary components of 0.000, 0.005, 0.010, 0.020, and 0.050. These values cover the refractive index range normally assumed to apply for atmospheric particulates in the mid-visible wavelength region, and the incremental steps in m are representative of the resolution that can be achieved by the fitting procedure for realistic amounts of noise.

Once an estimate of the optimal refractive index has been obtained by the least squares optimization procedure, a numerical inversion can be performed on the angular scattering data ($P_{11}(\theta)$ and $P_{22}(\theta)$), assuming this optimal refractive index value, to determine the unit volume particle size distribution. This unit volume size distribution should characterize the particulates in the volume of the atmosphere which was sampled by the bistatic lidar. A comparison can then be made between the columnar size distribution and the unit volume size distribution as a consistency check. The two size distributions should differ by only a constant scaling factor if the form of the unit volume size distribution and the particle refractive index are independent of altitude. These requirements can be expected to have been satisfied if S is constant with height (an indication of which, as was noted earlier, is provided by the predicted error level in S obtained from the solution procedure for determining S). If the inferred columnar and unit volume size distributions differ significantly in shape, it may be that the columnar size distribution is not a good estimate of the size distribution for the particulates at the altitude of the bistatic lidar scattering volume. In this case the columnar size distribution used in the optimization procedure could be considered to provide a first guess for the particle refractive index. The unit volume size distribution obtained with this first guess refractive index value could then be used in the optimization procedure to obtain an updated estimate of the refractive in-

TABLE 1. Normalized Values of the Performance Function Q for Simulated Data Case

m Real (n)	m Imaginary (κ)			
	0.000	0.005	0.010	0.020
1.54	23.10	8.67	3.01*	14.21*
1.50	9.97	1.84*	6.20	36.71
1.45	**1.00***	9.62	30.38	90.17
1.40	3.23	15.06	48.10	145.25
1.33	14.83			

Q values listed in the table are normalized by the minimum value of Q obtained from search, Q_{opt}. $Q_{opt} = 3.16 \times 10^{-3}$; $m_{opt} = 1.45 - 0.000i$; $\theta_i = 120°, 130°, 140°, 145°, 150°, 155°$, and 160°; $m_{true} = 1.50 - 0.005i$; $\Delta R_{l_r} \lesssim \pm 8\%$; $\Delta S \sim \pm 10\%$.

dex and so on (see discussion at the end of section 3). However, the inferred columnar and unit volume size distributions may differ from one another because of scattering effects by irregularly shaped particles and/or because the particles are not well characterized by a single, radius-independent refractive index value. If such is the case, it may be impossible to obtain a refractive index value and a spherical particle based size distribution that yield $P_{11}(\theta)$, $P_{22}(\theta)$, and S values which agree with the measurements.

3. Results and Discussion

To test the feasibility of the refractive index–size distribution retrieval method, it was first applied to simulated data sets generated for various aerosol size distribution models. The size distribution inversion obtained for one case (for zero measurement errors) is shown in Figure 3 along with the true distribution used to generate the simulated $\tau_p(\lambda)$ data employed in the inversion. The true distribution is a two-slope model [*Reagan et al.*, 1977*a*] given by

$$\frac{dN_c}{dr} = n_c(r) = C\,\frac{1 + (r/r_B)^{\nu_2+1}}{1 + (r/r_A)^{\nu_1+1}} \tag{9}$$

where C is a scaling constant and ν_1, ν_2, r_A, and r_B are shaping parameters. The name two-slope stems from the fact that the model can define two power law or Junge distribution regions, each region having a different slope (or effective ν value). This model can define distribution shapes which are similar to many of those determined for Tucson via both direct measurement and remote sensing methods [*Reagan et al.*, 1977*a*; *King et al.*, 1978].

Using the particular distribution parameter values given in Figure 3, (5) was evaluated by numerically integrating the Mie single-particle extinction cross sections over an assumed particle radius range from 0.02 to 10.0 μm. Values of $\tau_p(\lambda)$ were computed for the eight wavelengths which correspond to the center lines of the interference filters typically used in the University of Arizona solar radiometer, specifically, $\lambda = 0.37$, 0.44, 0.52, 0.61, 0.71, 0.78, 0.87, and 1.03 μm. A refractive index value of $m = 1.50 - 0.005i$ was used to calculate the simulated $\tau_p(\lambda)$ data, but the inversion was performed for an assumed value of $m = 1.45 - 0.000i$, which is the value typically used in the inversion procedure. The radius range over which the inversion was attempted was limited to 0.08–4.0 μm because the values of $\tau_p(\lambda)$ for the wavelengths given above are relatively unaffected by contributions from particles outside this radius range for representative particulate size distributions [*King et al.*, 1978].

It can be seen that the inversion reproduces the true distribution quite well even though the refractive index assumed for the inversion differed from that used to generate the simulated data. This is expected because, as was mentioned earlier, the shape of the size distribution obtained by inverting optical extinction data is not significantly affected by the value of refractive index assumed for the inversion. It should be noted that the inversion was performed with no noise added to the generated $\tau_p(\lambda)$ values to demonstrate clearly that assuming an incorrect refractive index value has only a minor effect on the inversion result. However, inversions were also performed with representative amounts of noise added to the generated $\tau_p(\lambda)$ values (i.e., with the addition of up to 4% rms Gaussian noise), and the inversions with and without noise were not greatly different from one another.

To test the refractive index grid search procedure, the columnar size distribution inversion result given in Figure 3 was used to compute the calculated values of $R_{lr}^{C}(\theta_i, m)$ and $S^{C}(m)$ required in (8). The experimental values of $R_{lr}^{E}(\theta_i)$ and S^{E} required in (8) were simulated by first computing these functions for the true size distribution (see Figure 3) and true refractive index ($m = 1.50 - 0.005i$) and then adding representative amounts of random noise. To generate the random errors in the simulated experimental values, 4% rms Gaussian noise was added to the computed values of $P_{11}(\theta_i)$ and $P_{22}(\theta_i)$, yielding an rms error in $R_{lr} = P_{11}/P_{22}$ of $\Delta R_{lr} \lesssim 8\%$, and 10% rms Gaussian noise was added to $P_{11}(\pi)$, yielding an rms error in $S = 1/P_{11}(\pi)$ of $\Delta S \sim 10\%$. The scattering angles θ_i used for this test case were ones typically selected for bistatic lidar experiments. They are included in Table 1, which lists the results of the grid search.

As can be seen in Table 1, the search procedure yielded an optimal refractive index estimate of $m_{opt} = 1.45 - 0.000i$, which differs somewhat from the true index value of $m_{true} = 1.50 - 0.005i$. This difference is due to the effect of noise included in the simulated experimental values. While the refractive index value determined by the search procedure was incorrect in this case, m_{opt} is an adjacent grid point to m_{true}, and the normalized performance function for m_{true} is the next smallest value (and thus defines the next most likely estimate of m). The tabular values also indicate the systematically decreasing trend in Q (as shown by the values with asterisks in the table) as m decreases. Specifically, there is a correlation between the real and imaginary components of m required to reduce Q such that as n is decreased, decreasing values of κ are required to achieve a further reduction in Q until a minimum is attained [*Byrne*, 1978].

Simulated data cases were also analyzed for Junge and log normal size distribution models. For noise levels in $R_{lr}(\theta)$ and S similar to those given in Table 1, m_{opt} obtained by the search procedure generally equaled the true refractive index value. When this was not the case, m_{opt} and m_{true} were adjacent grid points, as they were for the test case presented here. The trend of Q generally decreasing with decreasing m (until a minimum in Q is attained) as exhibited in Table 1 was also observed in the other test case results. For simulated data cases with no noise included in $R_{lr}(\theta)$ and S the search procedure always yielded m_{opt} equal to the true refractive index value. Thus the test case presented here represents a worst case result from our simulated data analyses.

The grid search results and refractive index determinations obtained for two real data cases are given in Tables 2 and 3 (which have formats similar to Table 1). The measurements were made with the University of Arizona combination bistatic-monostatic lidar system. The calculated values of $R_{lr}(\theta)$ and S used to determine the results in the tables were com-

TABLE 2. Normalized Values of the Performance Function Q for Data Collected in Tucson, Arizona, on November 20, 1974

	m Imaginary (κ)			
m Real (n)	0.000	0.005	0.010	0.020
1.54	9.50	4.82	2.77	1.38*
1.50	7.45	3.11	1.74	1.55
1.45	5.40	1.50	1.15*	2.84
1.40	5.57	**1.00***	1.35	5.38
1.33	4.75*			

Q values in the table are normalized by Q_{opt}. $Q_{opt} = 1.41 \times 10^{-2}$; $m_{opt} = 1.40 - 0.005i$; $\theta_i = 120°$, 130°, 135°, 140°, 145°, 148°, 151°, 153°, 155°, and 159°; $\Delta R_{lr} \sim \pm 17.5\%$; $\Delta S \sim \pm 16\%$.

TABLE 3. Normalized Values of the Performance Function Q for Data Collected in Tucson, Arizona, on May 26, 1976

m Real (n)	m Imaginary (κ)			
	0.000	0.005	0.010	0.020
1.54	2.63	2.07	2.24*	5.39*
1.50	1.50	2.03*	4.00	12.43
1.45	**1.00***	5.63	13.22	35.59
1.40	1.10	10.63	25.88	69.83
1.33	4.21			

Q values in the table are normalized by Q_{opt}. $Q_{opt} = 8.85 \times 10^{-2}$; $m_{opt} = 1.45 - 0.000i$; $\theta_i = 120°$, 130°, 140°, 145°, 150°, 155°, and 160°; $\Delta R_{l_r} \sim \pm 14\%$. $\Delta S \sim \pm 15\%$.

puted by using size distributions obtained by inverting solar radiometer measurements of $\tau_p(\lambda)$ collected close in time (within 12 hours or less) to the lidar observations. For November 20, 1974 (Table 2), m_{opt} was determined to be $1.40 - 0.005i$. The performance function appears to define a rather broad minimum in this case in that several values of Q are not much greater than Q_{opt}. Clearly, $m = 1.45 - 0.01i$ (an adjacent grid point to m_{opt}) should also be regarded as a probable solution because Q for this value of m is nearly as small as Q_{opt}. The results for May 26, 1976 (Table 3), appear to be more definitive, as the Q values for $m_{opt} = 1.45 - 0.000i$ and $m = 1.40 - 0.000i$ (for which Q is almost as small as Q_{opt}) are significantly smaller than Q for the other values of m. Thus for November 20, 1974, n is estimated to be between 1.40 and 1.45, while κ is estimated to be between 0.005 and 0.01. For May 26, 1976, n is also estimated to be between 1.40 and 1.45, and κ appears to be well determined by 0.000 (effectively zero).

The real refractive index components for these two cases might appear to be too low for an arid region like Tucson because common constituents of atmospheric particulates such as silicates, ammonium sulfate, and sodium chloride have real components in excess of 1.50 for relative humidities less than ~70% [*Junge*, 1963]. However, particles composed in part of sulfuric acid have rather low real refractive index components in the visible wavelength region even for very low relative humidites [*Palmer and Williams*, 1975]. Aircraft particulate measurements made on November 20, 1974 [*Reagan et al.*, 1977*a*] revealed that at least one third of the particulates were indeed sulfuric acid–water droplets, and $m \approx 1.40 - 0.000i$ is the appropriate refractive index for such particles at the in situ relative humidity measured by the aircraft (for ~35% relative humidity, $m \approx 1.40 - 0.000i$ at $\lambda = 0.7$ μm [*Palmer and Williams*, 1975]). Direct particulate measurements were not available on May 26, 1976, but we speculate that the low real refractive index component inferred for this occasion was also due to the presence of sulfuric acid in that measurements by *Charlson et al.* [1974, 1977], *Cunningham and Johnson* [1976], and *Trijonis* [1979] suggest that a significant fraction of atmospheric particulates over the United States may be composed of sulfate type particles. Most of the $R_{l_r}(\theta)$ data that we have extracted from other bistatic lidar measurements made in Tucson also indicate a low real refractive index component of 1.45 or less. The imaginary refractive index components inferred for the two real data cases (0.000 for May 26, 1976, and 0.005 → 0.001 for November 20, 1974) are within the range of those reported by *Grams et al.* [1974]. Analysis of S ratio data only (i.e., no $R_{l_r}(\theta)$ data available) obtained from slant path lidar measurements made in Tucson for several other days during the period 1975 and 1976 also yielded estimates of κ ranging between 0.000 and 0.008 [*Spinhirne*, 1977; *Spinhirne et al.*, 1980]. Thus the refractive index determinations obtained here for the two real data cases appear to be in good agreement with both direct aerosol measurements (when available) and other optical remote sensing inferences.

The particulate size distributions obtained for the real data cases cannot be validated by comparing them against known true distributions, as was done for the simulated data case. However, a consistency check can be made by inverting the angular scattering data (i.e., the $P_{11}(\theta)$ and $P_{22}(\theta)$ data), using the inferred refractive index m_{opt}, to obtain a size distribution that can be compared with the one obtained originally by inverting the $\tau_p(\lambda)$ data. Examples of this are shown in Figures 4 and 5 for the November 20, 1974, and May 26, 1976, data cases, respectively.

The numerical procedure which was used to perform the inversions of the $P_{11}(\theta)$ and $P_{22}(\theta)$ data is an adaptation of the constrained solution method proposed by *Phillips* [1962] and *Twomey* [1963]. Specifically, the procedure used to obtain the bistatic lidar results in Figures 4 and 5 is one first given by *Herman et al.* [1971] and revised by *Byrne* [1978]. It is similar to the optical depth inversion procedure used to invert the solar radiometer data [*King et al.*, 1978]. Since the size distributions obtained by inverting the solar radiometer data are columnar distributions, they had to be scaled in magnitude to be compared with the unit volume distributions obtained by inverting the bistatic lidar data. The scaling was done by selecting the multiplier constant (i.e., a reciprocal scale height) which gave best agreement, in a least squares sense, between the bistatic lidar measurements of $P_{11}(\theta)$ and $P_{22}(\theta)$ and theoretically computed values of the same functions computed for the radiometer-derived size distribution. The bistatic lidar size distribution inversions and the scaling constants obtained for

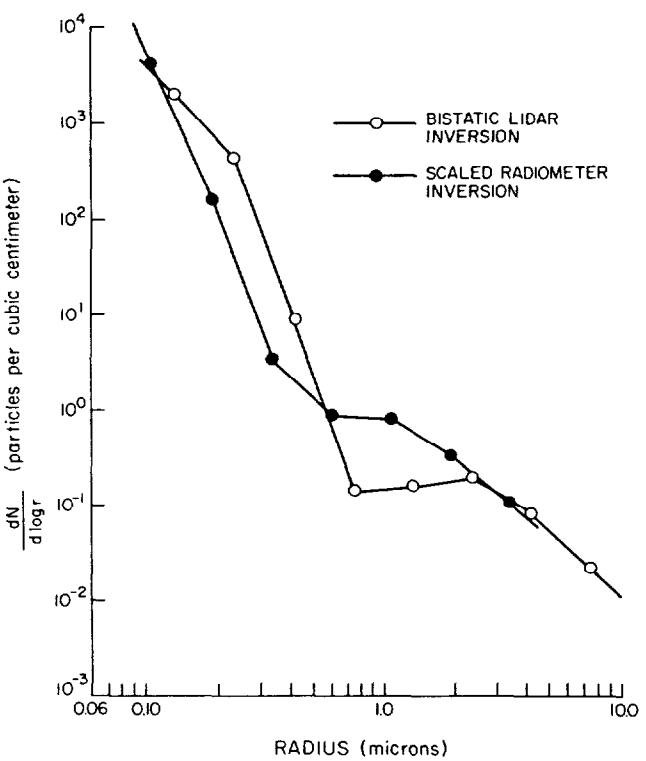

Fig. 4. Comparison of size distributions obtained by inverting solar radiometer and bistatic lidar measurements made in Tucson, Arizona, on November 20–21, 1974. The inversion of the bistatic lidar data is for $m = 1.40 - 0.005i$.

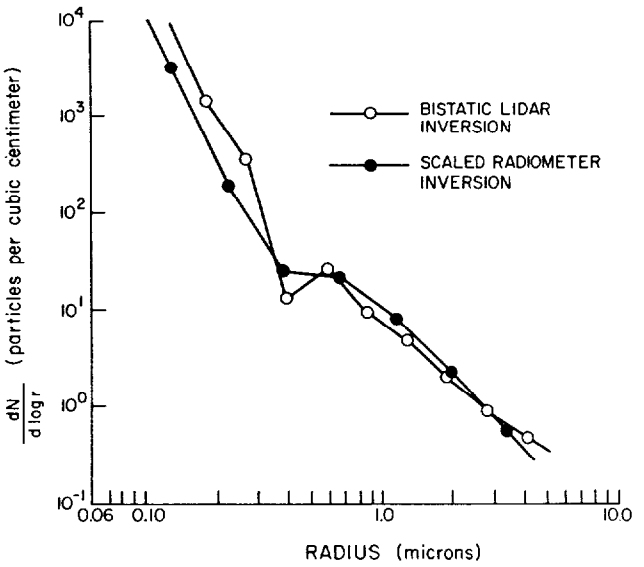

Fig. 5. Comparison of size distributions obtained by inverting solar radiometer and bistatic lidar measurements made in Tucson, Arizona, on May 26, 1976. The inversion of the bistatic lidar data is for $m = 1.45 - 0.000i$.

scaling the radiometer size distribution inversions were determined for $m = 1.40 - 0.005i$ for the November 20, 1974, case and for $m = 1.45 - 0.000i$ for the May 26, 1976, case (i.e., for the m_{opt} values obtained for each case).

It can be seen from the figures that the bistatic lidar and radiometer size distributions agree rather well with one another for each data case. The distributions obtained for November 20, 1974, agree favorably both with direct aircraft measurements made on that day and with model fit size distributions obtained from preliminary analyses of the lidar and radiometer data [*Reagan et al.*, 1977*a*]. The angular scattering measurements (bistatic lidar measurements) were also inverted for both data cases by using an assumed refractive index value of $m = 1.40 - 0.000i$. This yielded slightly poorer agreement between the bistatic lidar and radiometer size distributions for the May 26, 1976, case, but the agreement was as good, if not slightly better, for the November 20, 1974, case. The slight differences between the bistatic lidar (unit volume) and radiometer (columnar) size distributions may be a result of actual spatial inhomogeneities (both vertical and horizontal) in the physical properties of the particulates and/or nonspherical particle scattering effects. However, the combined effects of noise in the $\tau_\rho(\lambda)$, $R_\rho(\theta)$, and S data could also account for the observed differences between the bistatic lidar and radiometer size distributions. Thus further processing of the data does not appear warranted for these two sets of observations.

Given more accurate measurements, there are two refinements which could be included in the overall analysis procedure. First, improved estimates of m_{opt} could possibly be obtained by either determining Q for a finer mesh of grid points in m or by interpolating Q between the coarser grid points used to obtain the search results presented here. Second, the size distribution obtained by inverting the bistatic lidar data for the initial m_{opt} determination could be used in the refractive index search (in place of the radiometer size distribution) to obtain an updated estimate of m_{opt}. The new m_{opt} value could then be used to invert again the bistatic lidar data to obtain an updated size distribution, and the procedure could be iterated until some specified level of convergence was achieved. This latter suggestion might indeed yield improved results if the radiometer columnar size distribution and the bistatic lidar unit volume size distribution truly differed significantly from one another. In any case, inclusion of these iterative refinements should only be considered if the initial results appear significantly poorer than what one would expect from the quality of the data in question, because such iterations can greatly increase the computer time required for the analysis.

4. Summary and Conclusions

A method has been presented for remotely determining both the size distribution and the complex refractive index of atmospheric particulates from a combination of multiwavelength optical depth, angular scattering, and backscattering measurements. Results from both simulated and real solar radiometer and bistatic-monostatic lidar measurements have been given which demonstrate that the method can be applied with apparently good success even for rather large measurement errors. The results of two sets of actual observations have been shown to be self-consistent, and in one case the results were also substantiated by direct aircraft measurements. The refractive index determinations for these days revealed that the real component n can be significantly lower than the $1.5 \rightarrow 1.55$ range of values often assumed to apply for tropospheric particulates. In addition, the imaginary component of the refractive index, κ, was found to be rather small (~0.005 or less) but in fairly good agreement with several other determinations for the 0.5- to 0.7-μm wavelength range [*Ward et al.*, 1973; *Grams et al.*, 1974; *Lindberg and Laude*, 1974; *Carlson and Caverly*, 1977; *Spinhirne*, 1977; *Spinhirne et al.*, 1980]. The success with which the method was applied to actual observations, in spite of the particles being somewhat mixed in composition and not all perfect spheres [*Reagan et al.*, 1977*a*], indicates that using a combination of optical remote sensing techniques to determine the optical properties of particulates holds more promise than single-technique remote sensing approaches.

Acknowledgment. The research reported in this article has been supported by the Atmospheric Sciences Section of the National Science Foundation under grants ATM75-15551-A01 and ATM77-24493.

References

Ackerman, T., and M. B. Baker, Shortwave radiative effects of unactivated aerosol particles in clouds, *J. Appl. Meteorol., 16*, 63–69, 1977.

Byrne, D. M., Remote detection of atmospheric particulates using a bistatic lidar, Ph.D. dissertation, 144 pp., Univ. of Ariz., Tucson, 1978.

Carlson, T. N., and R. S. Caverly, Radiative characteristics of Saharan dust at solar wavelengths, *J. Geophys. Res., 82*, 3141–3152, 1977.

Chandrasekhar, S., *Radiative Transfer*, Dover, New York, 1960.

Charlson, R. J., A. H. Vanderpol, D. S. Covert, A. P. Waggoner, and N. C. Ahlquist, Sulfuric acid-ammonium sulfate aerosol: Optical detection in the St. Louis region, *Science, 184*, 156–158, 1974.

Charlson, R. J., A. H. Vanderpol, A. P. Waggoner, D. S. Covert, and M. B. Baker, The dominance of tropospheric sulfate in modifying solar radiation, in *Proceedings of the Symposium on Radiation in the Atmosphere*, pp. 32–36, Science, Princeton, N.J., 1977.

Cunningham, P. T., and S. A. Johnson, Spectroscopic observations of acid sulfate in atmospheric and particulate samples, *Science, 191*, 77–79, 1976.

Deirmendjian, D., *Electromagnetic Scattering on Spherical Polydispersions*, pp. 9–75, Elsevier, New York, 1969.

Eiden, R., The elliptical polarization of light scattered by a volume of atmospheric air, *Appl. Opt., 5*, 569–575, 1966.

Eiden, R., Determination of the complex index of refraction of spherical aerosol particles, *Appl. Opt., 10,* 749–754, 1971.

Fernald, F. G., B. M. Herman, and J. A. Reagan, Determination of aerosol height distributions by lidar, *J. Appl., Meteorol., 11,* 482–489, 1972.

Fymat, A. L., Inverse atmospheric radiative transfer problems: A nonlinear minimization search method of solution, *Phys. Earth Planet. Interiors, 12,* 273–282, 1976.

Grams, G. W., I. H. Blifford, Jr., D. A. Gillette, and P. B. Russell, Complex index of refraction of airborne soil particles, *J. Appl. Meteorol., 13,* 459–471, 1974.

Herman, B. M., S. R. Browning, and J. A. Reagan, Determination of aerosol size distributions from lidar measurements, *J. Atmos. Sci., 28,* 763–771, 1971.

Hodkinson, J. R., Light scattering and extinction by irregular particles larger than the wavelength, in *Electromagnetic Scattering,* edited by M. Kerker, pp. 87–100, Pergamon, New York, 1963.

Holland, A. C., and G. Gagne, The scattering of polarized light by polydisperse systems of irregular paticles, *Appl. Opt., 9,* 1113–1121, 1970.

Junge, C. E., The size distribution and aging of natural aerosols as determined from electrical and optical data on the atmosphere, *J. Meteorol., 12,* 13–25, 1955.

Junge, C. E., *Air Chemistry and Radioactivity,* Academic, New York, 1963.

King, M. D., Determination of the ground albedo and the index of absorption of atmospheric particulates by remote sensing, II, Application, *J. Atmos. Sci., 36,* 1072–1083, 1979.

King, M. D., and D. M. Byrne, A method for inferring total ozone content from the spectral variation of total optical depth obtained with a solar radiometer, *J. Atmos. Sci., 33,* 2242–2251, 1976.

King, M. D., and B. M. Herman, Determination of the ground albedo and the index of absorption of atmospheric particulates by remote sensing, I, Theory, *J. Atmos. Sci., 36,* 163–173, 1979.

King, M. D., D. M. Byrne, B. M. Herman, and J. A. Reagan, Aerosol size distributions obtained by inversion of spectral optical depth measurements, *J. Atmos. Sci., 35,* 2153–2167, 1978.

Kuriyan, J. G., D. H. Phillips, and M. T. Chahine, Multispectral extinction measurements to deduce the complex refractive index and the size distribution of aerosol particles, *J. Atmos. Sci., 31,* 2233–2236, 1974.

Lindberg, J. D., and L. S. Laude, Measurement of the absorption coefficient of atmospheric dust, *Appl. Opt., 13,* 1923–1927, 1974.

Palmer, K. F., and D. Williams, Optical constants of sulfuric acid; application to the clouds of Venus, *Appl. Opt., 14,* 208–219, 1975.

Perry, R. J., A. J. Hunt, and D. R. Huffman, Experimental determination of Mueller scattering matrices for nonspherical particles, *Appl. Opt., 17,* 2700–2710, 1978.

Phillips, D. L., A technique for the numerical solution of certain integral equations of the first kind, *J. Ass. Comput. Mach., 9,* 84–97, 1962.

Pinnick, R. G., D. E. Carroll, and D. J. Hofmann, Polarized light scattered from monodisperse randomly oriented nonspherical aerosol particles: Measurements, *Appl. Opt., 15,* 384–393, 1976.

Pollack, J. B., and J. N. Cuzzi, Scattering by non-spherical particles of size comparable to a wavelength: A new semiempirical theory, in *Reprints of 3rd Conference on Atmospheric Radiation,* pp. 20–23, American Meteorological Society, Boston, Mass., 1978.

Reagan, J. A., and B. M. Herman, Bistatic lidar investigations of atmospheric aerosols, in *Preprints 14th Conference Radar Meteorology,* pp. 275–280, American Meteorological Society, Boston, Mass., 1970.

Reagan, J. A., D. M. Byrne, B. M. Herman, and M. D. King, Determination of the complex refractive index of aerosol particles from bistatic lidar and solar radiometer measurements, in *Proceedings of the Topical Meeting on Atmospheric Aerosols: Their Optical Properties and Effects,* pp. TuC3-1–TuC3-4, Optical Society of America, Washington, D. C., 1976.

Reagan, J. A., J. D. Spinhirne, D. M. Byrne, D. W. Thomson, R. G. dePena, and Y. Mamane, Atmospheric particulate properties inferred from lidar and solar radiometer observations compared with simultaneous in situ aircraft measurements: A case study, *J. Appl. Meteorol., 16,* 911–928, 1977*a*.

Reagan, J. A., D. M. Byrne, M. D. King, and B. M. Herman, Combined optical techniques for remotely determining both the size distribution and complex refractive index of atmospheric particulates, in *Proceedings of the Fourth Joint Conference on Sensing of Environmental Pollutants,* pp. 554–560, American Chemical Society, Washington, D. C., 1977*b*.

Russell, P. B., W. Viezee, R. D. Hake, Jr., and R. T. H. Collis, Lidar observations of the stratospheric aerosol: California, October 1972 to March 1974, *Quart. J. Roy. Meteorol. Soc., 102,* 675–695, 1976.

Shaw, G. E., J. A. Reagan, and B. M. Herman, Investigations of atmospheric extinction using direct solar radiation measurements made with a multiple wavelength radiometer, *J. Appl. Meteorol., 12,* 374–380, 1973.

Spinhirne, J. D., Monitoring of tropospheric aerosol optical properties by laser radar, Ph.D. dissertation, 176 pp., Univ. of Ariz., Tucson, 1977.

Spinhirne, J. D., J. A. Reagan, and B. M. Herman, Vertical distribution of aerosol extinction cross section and inference of aerosol imaginary index in the troposphere by lidar technique, *J. Appl. Meteorol., 19,* in press, 1980.

Trijonis, J., Visibility in the southwest—An exploration of the historical data base, *Atmos. Environ., 13,* 833–843, 1979.

Twitty, J. T., R. J. Parent, J. A. Weinman, and E. W. Eloranta, Aerosol size distributions: Remote determination from airborne measurements of the solar aureole, *Appl. Opt., 15,* 980–989, 1976.

Twomey, S., On the numerical solution of Fredholm integral equations of the first kind by the inversion of the linear system produced by quadrature, *J. Ass. Comput. Mach., 10,* 97–101, 1963.

Twomey, S., Pollution and the planetary albedo, *Atmos. Environ., 8,* 1251–1256, 1974.

Twomey, S., The influence of pollution on the shortwave albedo of clouds, *J. Atmos. Sci., 34,* 1149–1152, 1977.

van de Hulst, H. C., *Light Scattering by Small Particles,* John Wiley, New York, 1957.

Ward, G., K. M. Cushing, R. D. McPeters, and A. E. S. Green, Atmospheric aerosol index of refraction and size-altitude distribution from bistatic laser scattering and solar aureole measurements, *Appl. Opt., 12,* 2585–2592, 1973.

Yamamoto, G., and M. Tanaka, Determination of aerosol size distribution from spectral attenuation measurements, *Appl. Opt., 8,* 447–453, 1969.

Zerull, R. H., and R. H. Giese, Microwave analogue studies, in *Planets, Stars, and Nebulae Studies With Photopolarimetry,* edited by T. Gehrels, pp. 901–915, University of Arizona Press, Tucson, 1974.

Zerull, R. H., and K. Weiss, Scattering properties of irregular dielectric and absorbing particles, in *Proceedings of the Topical Meeting on Atmospheric Aerosols: Their Optical Properties and Effects,* pp. MC10-1–MC10-3, Optical Society of America, Washington, D. C., 1976.

(Received July 2, 1979;
revised November 26, 1979;
accepted December 17, 1979.)